

# Polytelluride square planar chain induced anharmonicity results in ultralow thermal conductivity and high thermoelectric efficiency in $\text{Al}_2\text{Te}_5$ monolayers

Iraj Maleki<sup>1</sup>, S. Mehdi Vaez Allaei<sup>1,2\*</sup>, and S. Shahab Naghavi<sup>3\*</sup>

<sup>1</sup>Department of Physics, University of Tehran, Tehran 14395-547, Iran

<sup>2</sup>New Uzbekistan University, Movarounnahr Street 1, Tashkent 100000, Uzbekistan

<sup>3</sup>Shahid Beheshti University, Department of Physical and Computational Chemistry, Shahid Beheshti University, G.C., Evin, 1983969411 Tehran, Iran

E-mail: [smvaez@ut.ac.ir](mailto:smvaez@ut.ac.ir)

E-mail: [s\\_naghavi.sbu.ac.ir](mailto:s_naghavi.sbu.ac.ir)

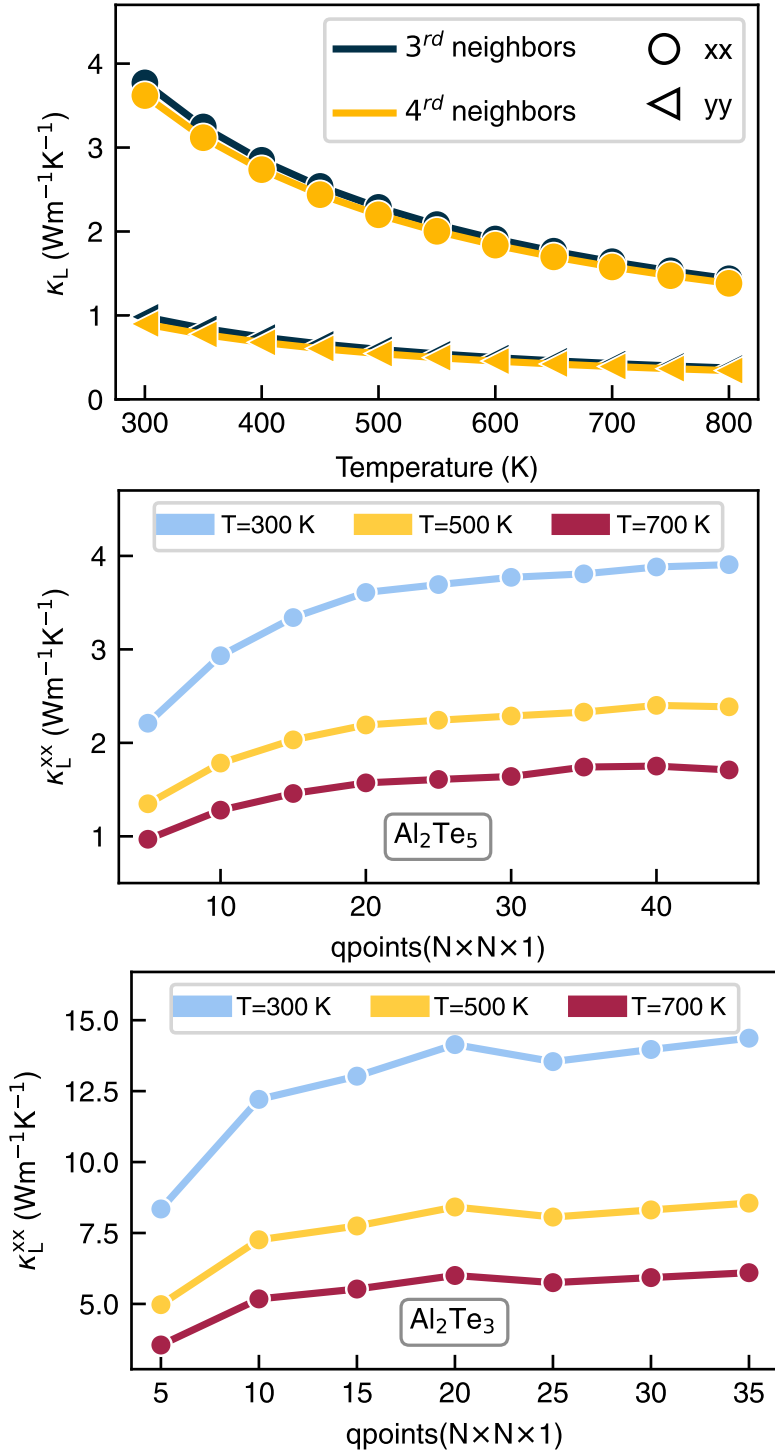
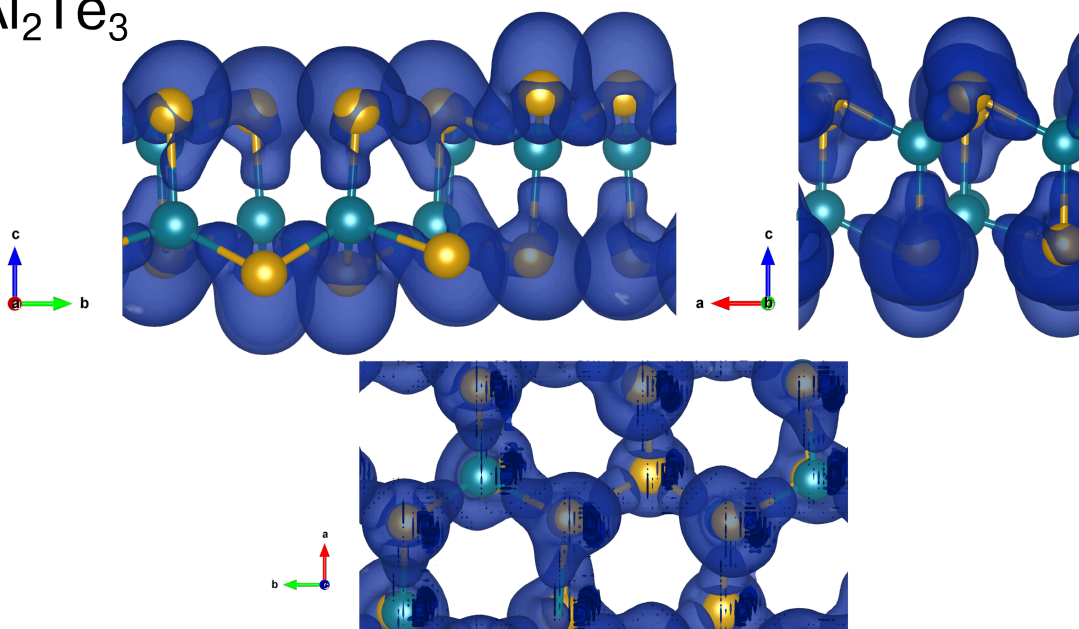


**Fig S1:** Convergence test for  $\kappa_L$  as function of q-point grid and interaction cutoff.

$\text{Al}_2\text{Te}_3$



$\text{Al}_2\text{Te}_5$

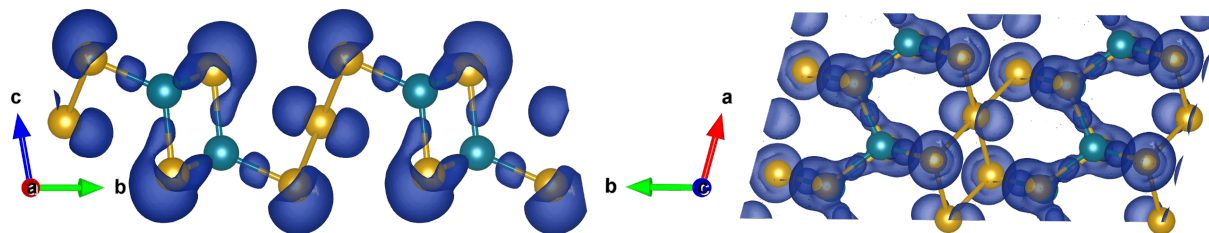


**Fig S2:** Electron localization function (ELF) plots of  $\text{Al}_2\text{Te}_3$  and  $\text{Al}_2\text{Te}_5$  from different viewpoints.

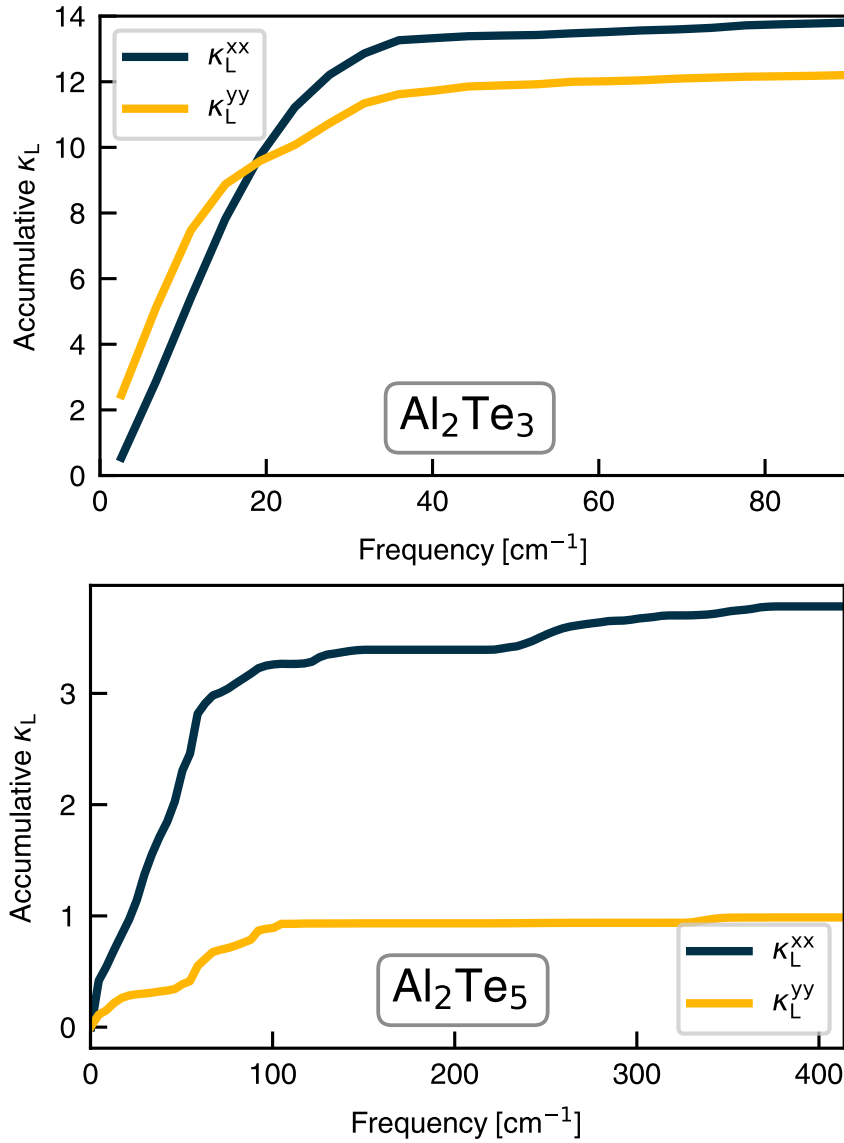


**Fig S3:** Accumulative  $\kappa_L$  versus frequency for  $\text{Al}_2\text{Te}_3$  and  $\text{Al}_2\text{Te}_5$  at 300K. The figure reveals that lattice thermal transport is dominated by phonon modes with frequencies less than  $40 \text{ cm}^{-1}$  and  $100 \text{ cm}^{-1}$  for  $\text{Al}_2\text{Te}_3$  and  $\text{Al}_2\text{Te}_5$ , respectively.



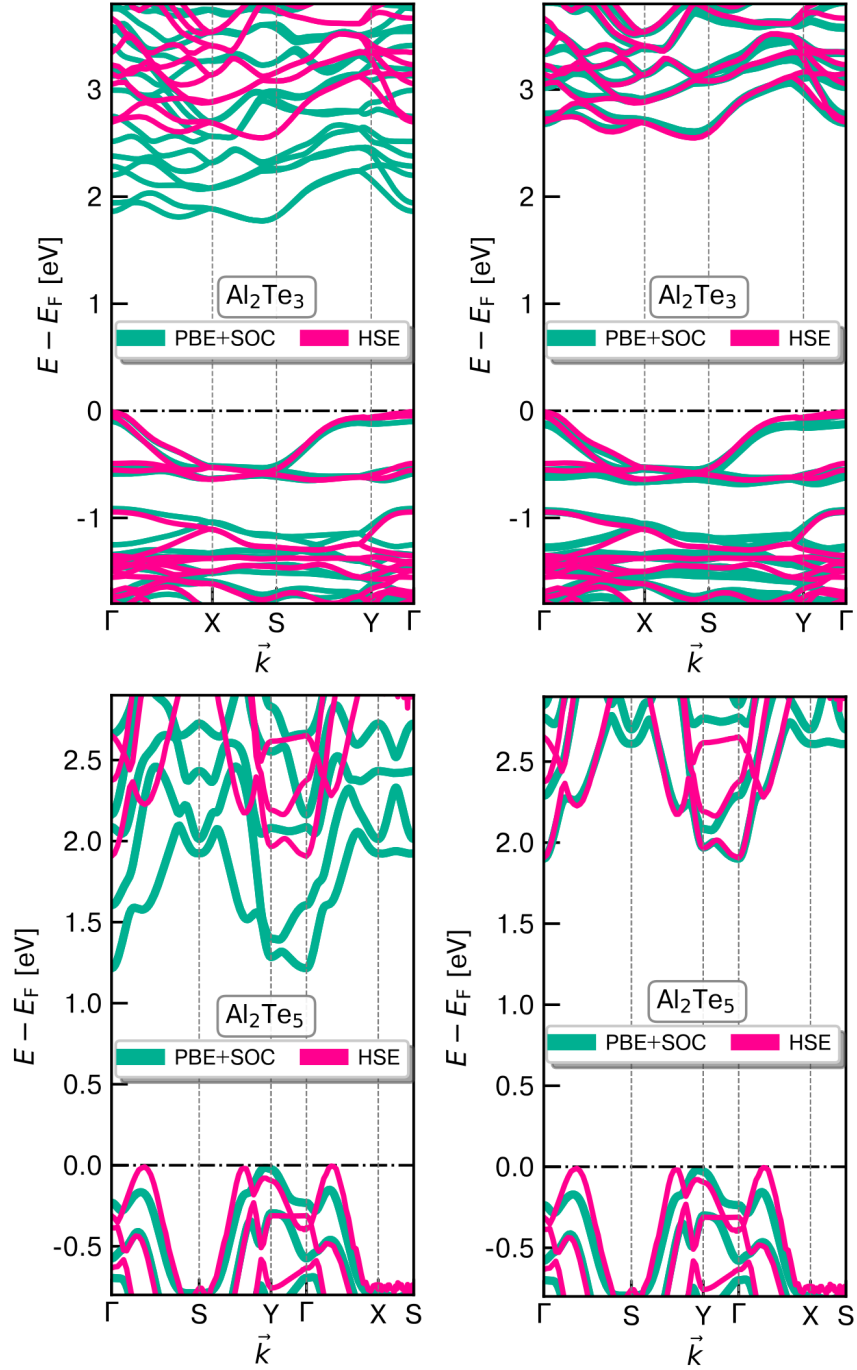


**Fig S4:** Overlay of the HSE and PBE+SOC band structures of  $\text{Al}_2\text{Te}_3$  and  $\text{Al}_2\text{Te}_5$ . To simplify the comparison, the right panel shifts the PBE band gap by 0.697 eV for  $\text{Al}_2\text{Te}_3$  and 0.651 eV for  $\text{Al}_2\text{Te}_5$ . The HSE-calculated band structure of  $\text{Al}_2\text{Te}_5$  exhibits enhanced valley degeneracy and changes in band curvature, while its CB and also that of  $\text{Al}_2\text{Te}_3$  remains similar to the PBE-calculated one.

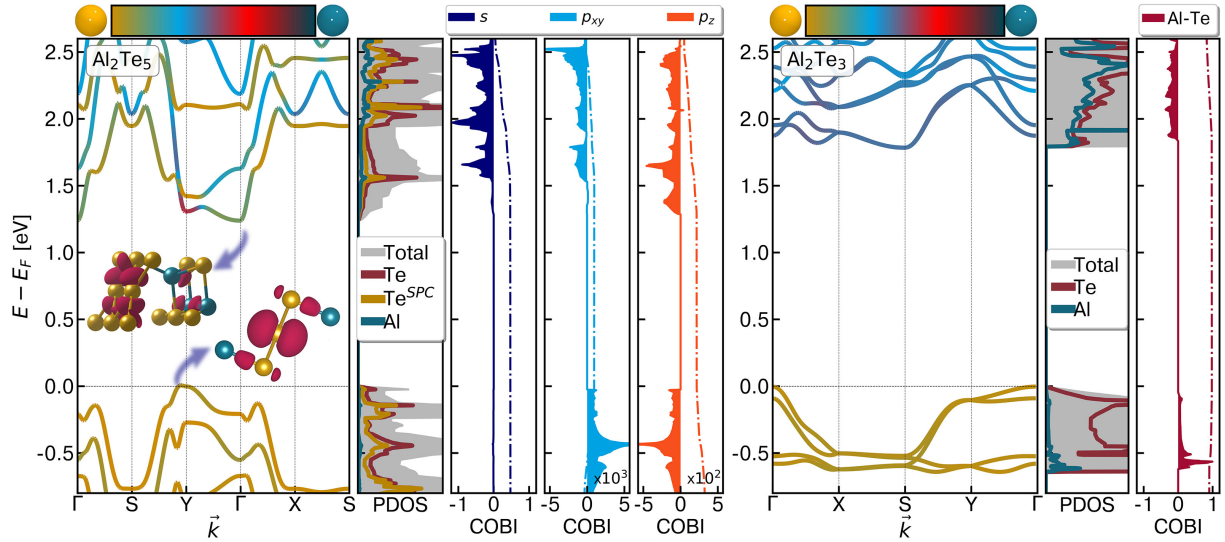


**Fig S5:** PBE+SOC functional atom-projected band structures, density of states, and COBI plots for  $\text{Al}_2\text{Te}_5$  (left panel) and  $\text{Al}_2\text{Te}_3$  (right panel). The inset in the band structure plot of  $\text{Al}_2\text{Te}_5$  depicts the charge decomposition of the valence band maximum (VBM) and conduction band minimum (CBM).

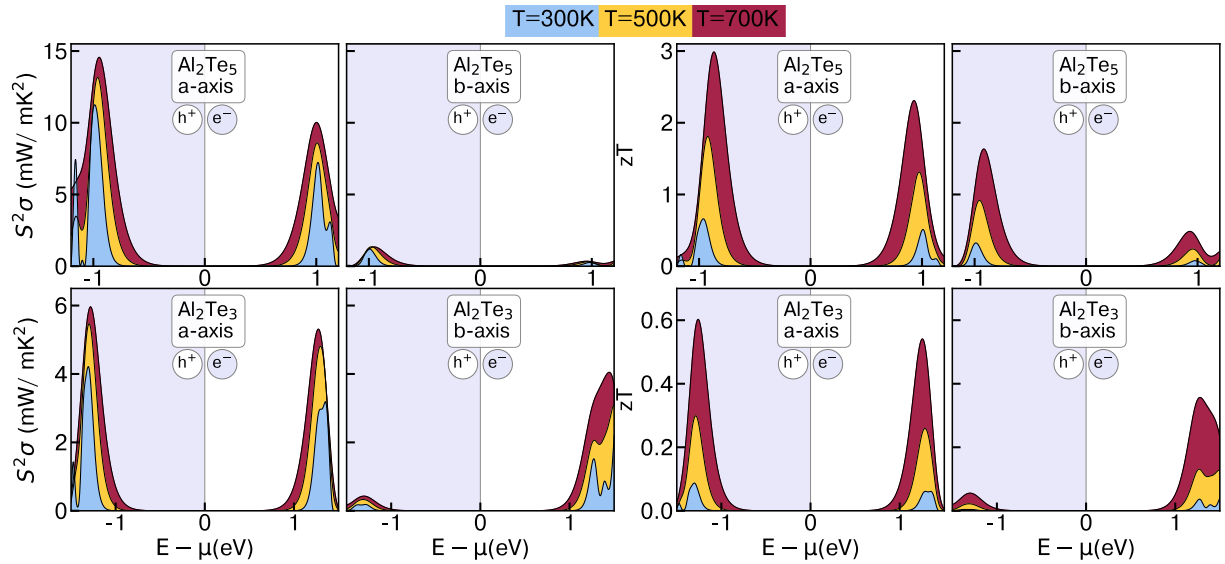


**Fig S6:** Thermoelectric properties of  $\text{Al}_2\text{Te}_5$  and  $\text{Al}_2\text{Te}_3$  along the a- and b-axes were calculated using the HSE functional and the constant relaxation time approximation (CRTA) with a relaxation time of  $\tau = 1 \times 10^{-14}\text{s}$ .

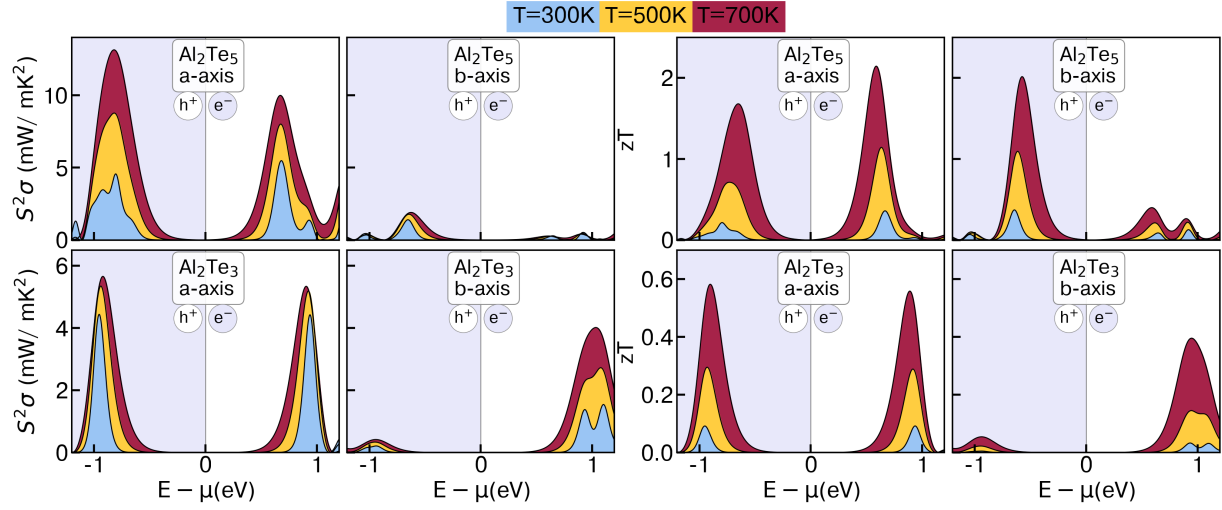


**Fig S 7:** The electron and hole thermoelectric properties of  $\text{Al}_2\text{Te}_5$  and  $\text{Al}_2\text{Te}_3$  along the a- and b-axes were calculated using the PBE+SOC functional and the constant relaxation time approximation (CRTA) with a relaxation time of  $\tau = 1 \times 10^{-14}\text{s}$ .

**Table S 1:** The high symmetry k-points coordinates used for representation band structure and phonon dispersion.

	Lable	$k_x$	$k_y$	$k_z$
$\text{Al}_2\text{Te}_5$	$\Gamma$	0.0000	0.0000	0.0000
	S	0.5000	0.5000	0.0000
	X	0.5000	0.0000	0.0000
	Y	0.0000	0.5000	0.0000
$\text{Al}_2\text{Te}_3$	$\Gamma$	0.0000	0.0000	0.0000
	X	0.5000	0.0000	0.0000
	S	0.5000	0.5000	0.0000
	Y	0.0000	0.5000	0.0000

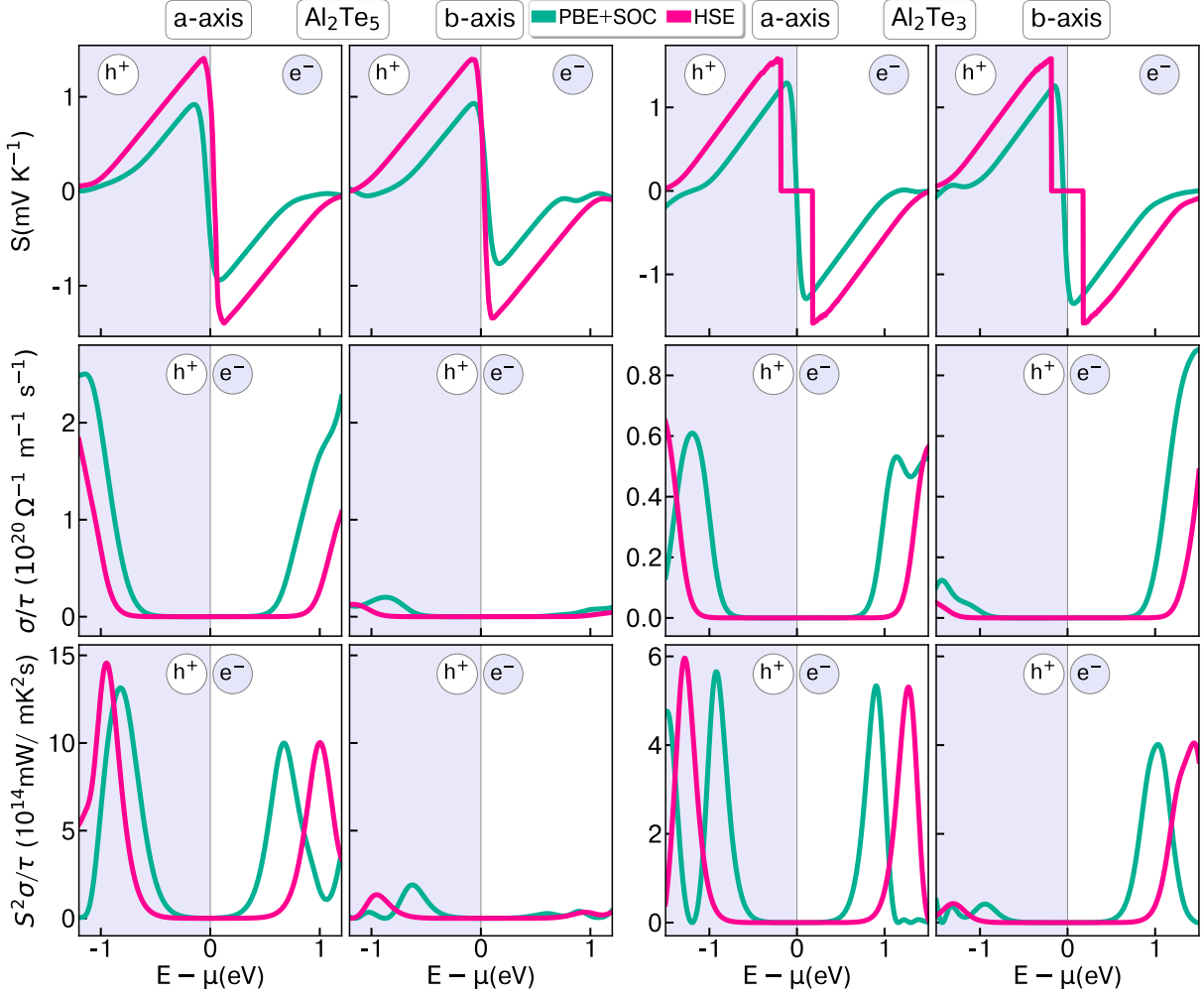


**Fig S8:** Calculated Seebeck coefficients ( $S$ ), electrical conductivity ( $\sigma$ ), and power factor (PF) of  $\text{Al}_2\text{Te}_5$  and  $\text{Al}_2\text{Te}_3$  using PBE and HSE methods at 700K. The HSE-calculated  $S$  is larger than that of PBE due to its dependence on the band gap. However, if the band gap widens, akin to the scissor operator, the enhancement of  $S$  and  $\sigma$  counterbalances, leaving  $PF$  unchanged—a critical factor for determining  $zT$ .  $\text{Al}_2\text{Te}_3$  exemplifies this behavior. However, in  $\text{Al}_2\text{Te}_5$ , HSE alters the band curvature and increases the valley degeneracy of VB, slightly enhancing the  $p$ -type  $PF$  while leaving the CB and  $n$ -type  $PF$  unchanged.

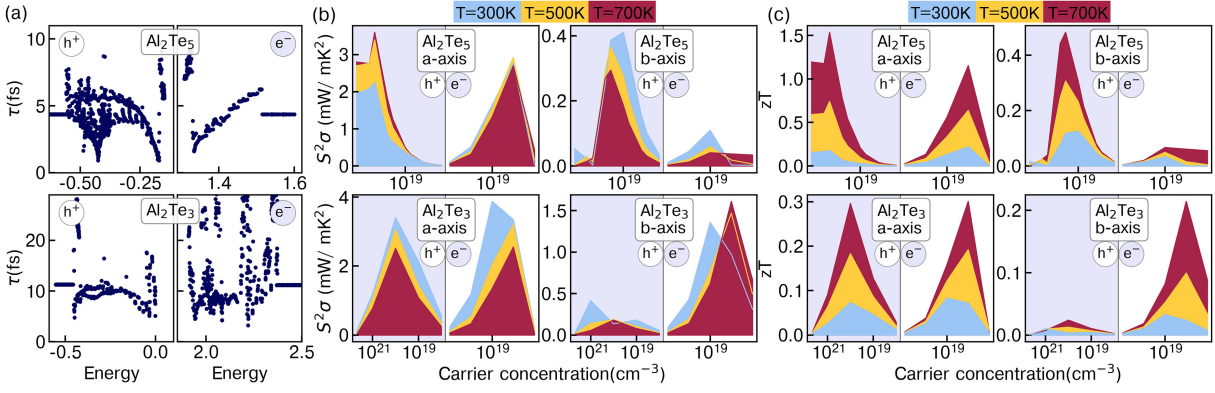


**Fig S9:** The electron and hole thermoelectric properties of  $\text{Al}_2\text{Te}_5$  along the a- and b-axes were calculated using the PBE+SOC functional and accurate relaxation time that contain all scattering rates.

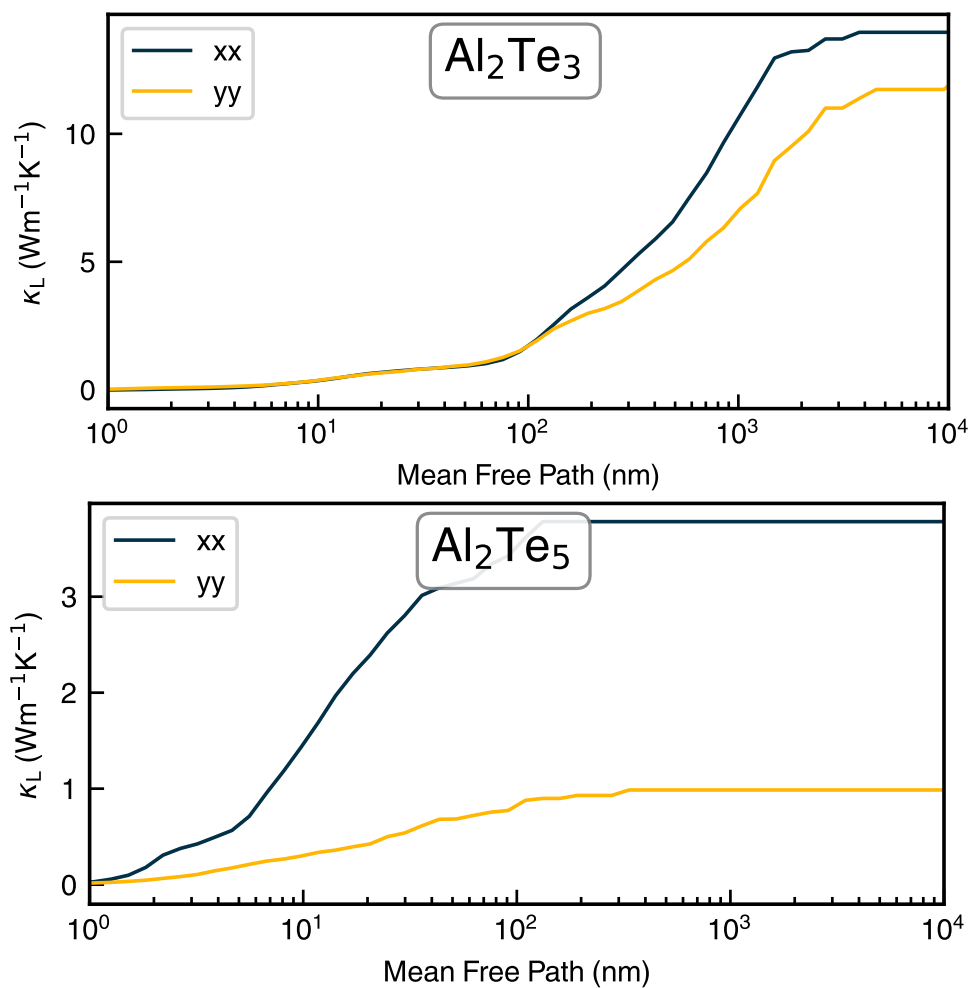


**Fig S10:** Accumulative  $\kappa_L$  versus mean free path for  $\text{Al}_2\text{Te}_3$  and  $\text{Al}_2\text{Te}_5$  at 300K. As the figure illustrates, lattice thermal transport could decrease by half with nanostructuring at sizes of approximately 500 nm and 50 nm for  $\text{Al}_2\text{Te}_3$  and  $\text{Al}_2\text{Te}_5$ , respectively.

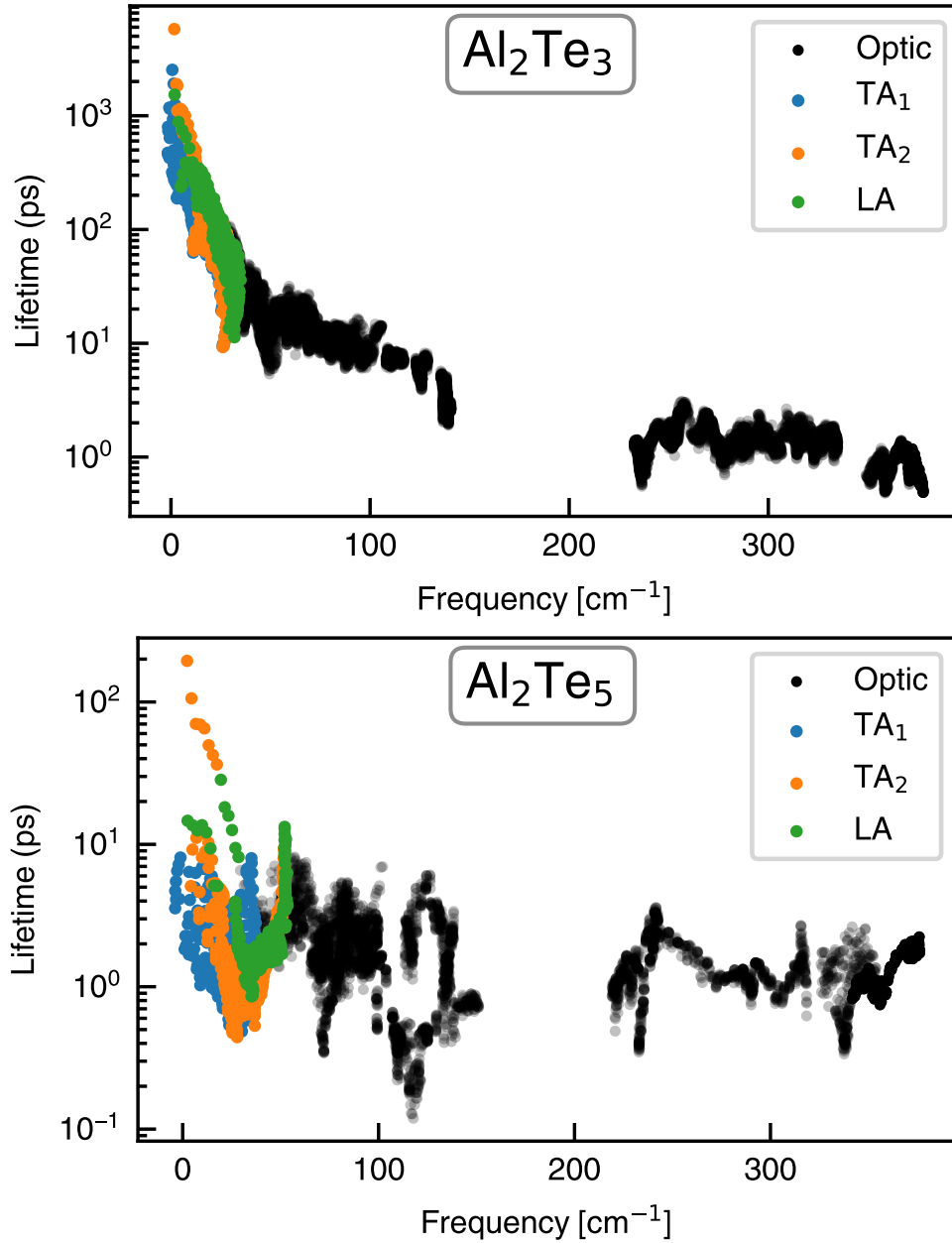


**Fig S11:** The calculated phonon lifetimes correspond to the phonon frequency at 300K for both materials. As the figures clearly depict, the phonon lifetime for  $\text{Al}_2\text{Te}_5$  is almost one order of magnitude lower than that for  $\text{Al}_2\text{Te}_3$ , resulting in higher scattering rates and lower phonon thermal transport in  $\text{Al}_2\text{Te}_5$ .